AERODYNAMIC ENHANCEMENT IN INNER CHANNEL OF TURBINE BLADE

PIOTR KACZYŃSKI, RYSZARD SZWABA,
BARTOSZ PUCHOWSKI, PIOTR DOERFFER
AND PAWEŁ FLASZYŃSKI

Institute of Fluid-Flow Machinery, Polish Academy of Sciences
Fiszera 14, 80-952 Gdansk, Poland

(received: 5 January 2015; revised: 11 February 2015;
accepted: 20 February 2015; published online: 20 March 2015)

Abstract: This paper presents the numerical and experimental study of the flow structure in a radial cooling passage model of a gas turbine blade. The investigations focus on the flow aerodynamics in the channel, which is an accurate representation of the configuration used in aero engines. The flow structure and pressure drop were measured by classical measurement techniques. The stagnation pressure and velocity measurements in a channel outlet plane were performed. The investigations concerning the flow field and heat transfer used in the design of radial cooling passages are often developed from simplified models. It is important to note that real engine passages do not have perfect rectangular cross sections, but include corner fillets, ribs with fillet radii and special orientation. Therefore, this work provides detailed fluid flow data for a model of radial cooling geometry which possesses very realistic features. The main purpose of these investigations was to study different channel configurations and their influence on the flow structure and pressure losses in a radial cooling passage of a gas turbine blade.

Keywords: turbine blade, internal channel, radial passage, blade cooling

1. Introduction

Heat exchange is a critical issue in the development of gas turbine blades. Gas temperature at the first stage of the turbine is extremely high and can cause metal melting, thus intensive cooling of the NGV and first blades is absolutely necessary. Usually a combination of internal convection cooling and film cooling is applied. They have to be designed for high efficiency, long life cycles and safe operation in spite of being exposed to high thermal loadings of the engine.

The internal cooling systems of high pressure blades in modern aero engines are very complex and essentially rely on serpentine systems. The data available for the design tends to be in the form of correlations obtained from a large number of idealised geometries, *e.g.* [1–3] over restricted ranges of operation. The work

described in the present paper was a part of the work undertaken within the EU ERICKA project [4]. The project concerned the generation of test data on the heat transfer and pressure drop performance of ribbed cooling passages which, together with CFD and optimisation tools, is intended to support the development of more effective cooling systems for rotating turbine components.

Correlations for the heat transfer coefficient and pressure drop used in the design of radial cooling passages are often developed from data gained from simplified, flat surfaced models over specific conditions [5]. It is important to note that real engine passages do not have perfect rectangular cross-sections, but include fillets and space oriented ribs also with fillets. Therefore, this work provides detailed fluid flow data for a model of radial cooling geometry which possesses very realistic features. The ribs are of a real shape.

The main goal of this paper is to study the flow structure in three different configurations of the radial cooling passage model of a gas turbine blade. The basic (reference) configuration of the measurement channel characterises the 1:4 cross section aspect ratio and parallel settings of ribs on the upper and lower walls. Based on the reference channel, two directions of modifications of this configuration are proposed to enhance the aerodynamic performance, *i.e.* to achieve a lower pressure drop what directly results in lower aerodynamic losses. A better cooling system means that the amount of cooling air that needs to be sent to the turbine is reduced. Reducing the cooling flow increases the efficiency of the turbine stage and also has a direct benefit on the efficiency of the cycle.

The idea of the first channel modification is shown in Figure 1. As one can see the parallel ribs (Figure 1a) generate two counter-rotating vortices. Changing the inclination of the ribs on the opposite wall (Figure 1b) we receive the so called crossing setting of ribs in the channel. This rib configuration is the reason why one main vortex, flowing over the whole circumference, is created in the channel. The second direction to enhance the channel aerodynamic performance is to increase the cross section aspect ratio to 1:6. At the same the Reynolds number this configuration may also bring the lower aerodynamic losses. Such a high aspect ratio can be implemented in heavy loaded turbine blades, as such application is allowed by their design.

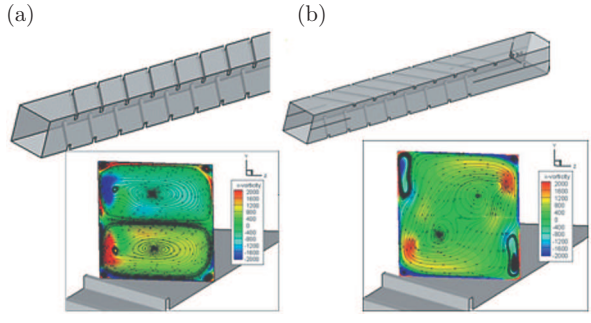

Figure 1. Rib settings in channel flow

2. Experimental Setup

The view of the test section is shown in Figure 3. This test section corresponds to an internal radial passage channel of a turbine blade. The lower and upper walls are ribbed, what corresponds to the pressure and suction sides of the turbine blade inner channel. In the downstream view the left side wall corresponds to the leading edge (LE) direction, the right side wall corresponds to the trailing edge (TE) direction. Small ribs located on the lower (PS) and upper (SS) walls have parallel and crossing setting to each other. The ribs were skewed by 45 deg in relation to the flow direction. The aspect ratios (AR) of the channel were 1:4 and 1:6 (for parallel ribs only). The channel width was 20 mm. The Reynolds number in the experiment based on the hydraulic diameter was $\mathrm{Re} = 63\,000$. Together it gives three measurement cases and the nomenclature for particular flow cases which will be used in the paper and are shown in Table 1.

Table 1. Measurement cases and nomenclature

	Aspect ratio	
Ribs setting	1:4	1:6
Parallel	Par-1:4	Par-1:6
Crossing	Cr-1:4	

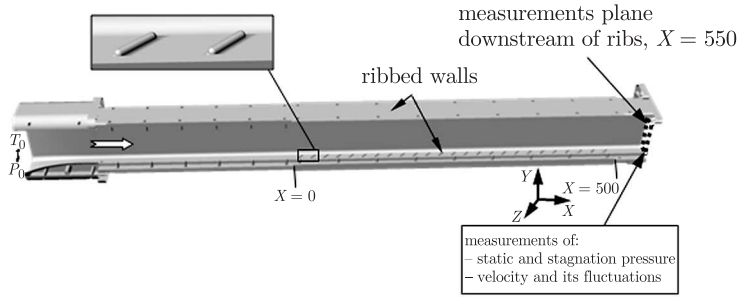

Figure 2. View of test section

The flow structure and pressure drop were measured by classical measurements techniques. At the test channel inlet the stagnation pressure and temperature were measured by means of a barometer and a thermocouple. The ribbed section spreads in the channel between coordinates $X = 0$ and $X = 500$ mm. The static pressure along the channel was measured by pressure taps. The stagnation pressure and velocity were measured in the channel outlet plane $X = 550$. The stagnation pressure downstream of ribs was measured with a Pitot probe. The velocity was measured with a hot wire probe. The wire of the probe was set parallel to the lower and upper walls, hence the 2D XY velocity magnitude was registered in such configuration. Obviously the longitudinal (X) component is predominating.

Moreover, the boundary layer velocity profile for Par-1:4 flow case was measured upstream of the ribbed section at $X = -50$ mm. The centre of the first

rib in the test section is located at $X = 10$. Thus, the profiles were measured 60 mm upstream of the ribs.

The measurement accuracy of the barometer is about ±15 Pa. All the measured pressures, both static and stagnation, in the test section were measured with a pressure scanner – PSI NetScaner 9116 with a range of 2500 Pa. The measurement accuracy of the scanner is ±1.5 Pa. The velocity fluctuations were measured with a DANTEC Streamline® Constant Temperature Anemometry (CTA) system.

In the parallel rib configuration there were 25 and 24 ribs on the lower and upper walls, respectively. Thus, the ribs on the upper wall are shifted half a pitch in relation to the lower wall. In the crossing configuration the number of ribs on the lower and upper walls is the same – 24.

3. Numerical model description

3D numerical simulations were performed using the commercial Ansys Fluent code. The turbulence model k-ω SST was used in the calculations which was a compromise between the computational resources and satisfactory numerical results. The third order MUSCL scheme was used for spatial discretization.

The mass flow inlet was used as the inlet boundary condition for the channel with the aspect ratios 1:4 and 1:6. The mass flow rate was fitted to the experimental data. The turbulent intensity at the given hydraulic diameter was equal to 1% and the inlet flow temperature was 297.15 K for all cases. The geometry of the test section including the inlet, the ribbed sections and the outlet box is shown in Figure 3. The symmetry conditions were implemented for the third part of the test section which is called the outlet box. The boundary condition at the outlet was ambient pressure of 101 325 Pa.

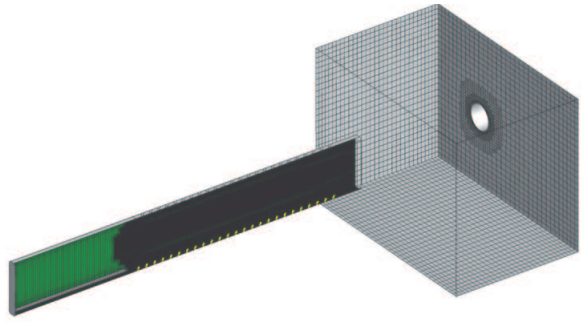

Figure 3. Computational domain

A computational mesh was created using the Hexpress/Numeca software. The computational domain is an accurate representation of the experimental test section and the mesh contains about 7 million elements. The unstructured hexahedral mesh was refined in the ribbed part of the channel (Figure 3). An especially high number of refinements are around the ribs where stagnations areas

and high velocities can be observed (Figure 4). Moreover, this region is critical because ribs introduce and develop a vortex structure in the flow. A high level of refinements gives sufficient prediction of the flow structure. The refined mesh close to the wall keeps the parameter $y \pm 1$ in the ribbed and inlet sections.

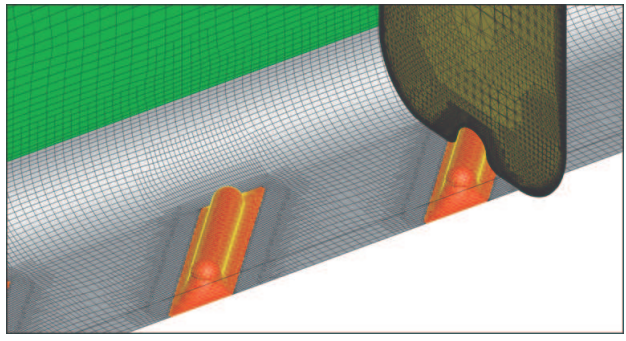

Figure 4. Mesh on ribbed wall and in channel cross-section

4. Numerical results and comparison of experimental data

In order to predict the proper flow structure in the channel the first step at the beginning of the numerical simulation was to compare some flow features obtained from CFD with experimental data.

A comparison of the static pressure distributions along the channel for all three flow cases is shown in Figure 5. In this figure one can notice that the static pressure at the inlet and outlet of the ribbed test section is properly predicted. Discrepancies between experimental data and numerical results can be noticed within the middle part of the ribbed channel. A similar trend appears as well in the channel of 1:4 AR and 1:6 AR. It can be a result of different boundary layer profile (Figure 6) development between the CFD and the experiment. In

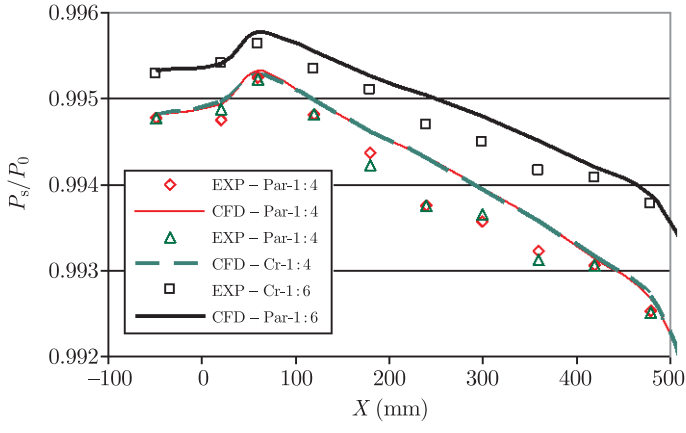

Figure 5. Static pressure distribution along test section

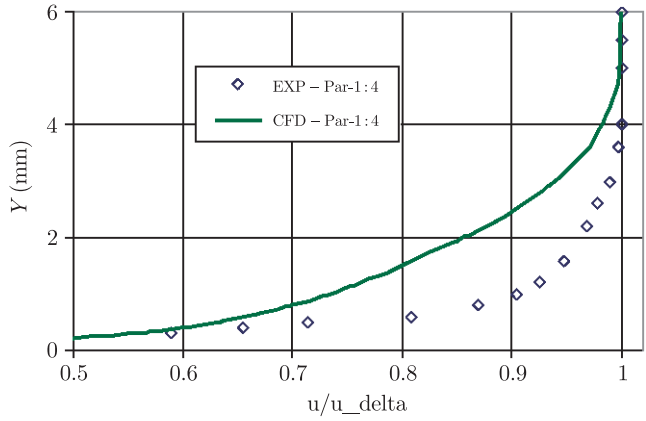

Figure 6. Boundary layer velocity profile upstream of ribbed section

a numerical simulation there was no transition model applied (the turbulent boundary layer is assumed along the whole test section length) and the inlet part of the channel (convergent nozzle) is not included in the model. Therefore, the discrepancies between the CFD and the experiment at the inlet are quite natural. The shape parameter H12 of the boundary layer in the experiment is equal to 2.0, which indicates that it is a transition layer. Discrepancies in the middle part of the channel are probably caused by a different vortex development prediction near the wall by the turbulence model in CFD with regards to the experiment.

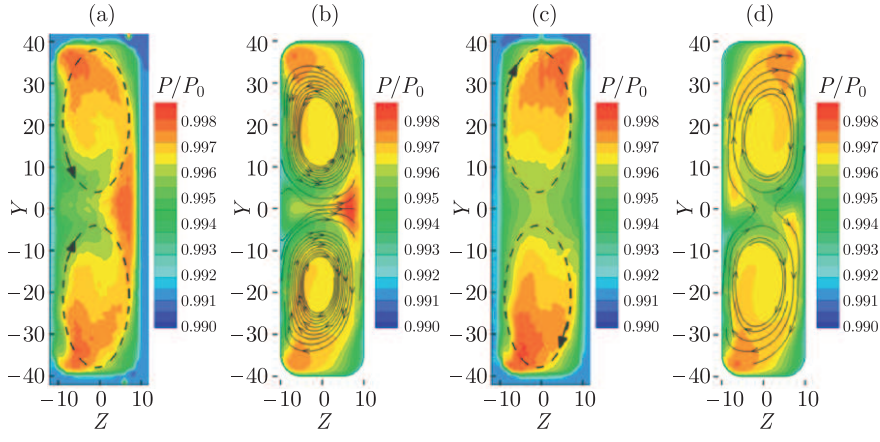

Figure 7. Comparison of stagnation pressure distributions at channel outlet ($X = 550$) for 1:4 AR, (a) EXP-Par, (b) CFD-Par, (c) EXP-Cr, (d) CFD-Cr

Comparisons of numerical and experimental results of normalised stagnation pressure in the plane 50 mm ($X = 550$) downstream of the ribbed section for the channel of 1:4 AR are shown in Figures 7–8. Figures 7a, 8a and 7b, 8b show the results for parallel rib configuration, Figures 7c and 7d for crossing rib setting. The coordinates $Y = 0$ and $Z = 0$ are assumed in the middle of the channel as is

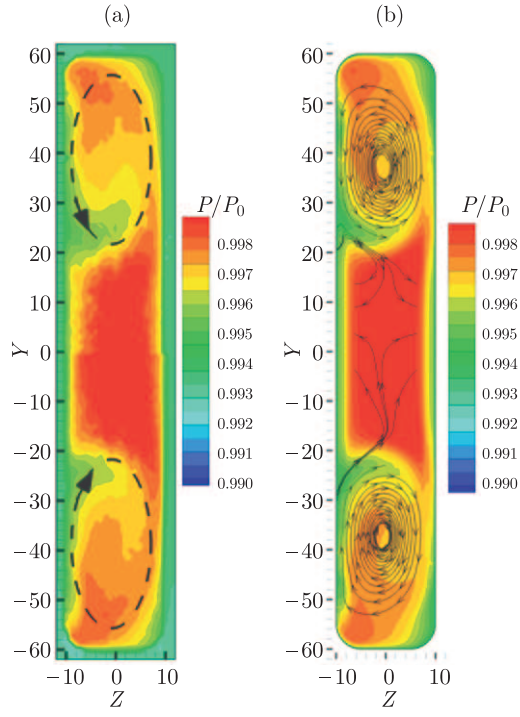

Figure 8. Comparison of stagnation pressure distributions at channel outlet ($X = 550$) for 1:6 AR, (a) EXP-Par, (b) CFD-Par

displayed in Figures 7–8. The results are presented according to the downstream view of the flow. The dashed ellipses with an arrow on the experimental results indicate the sense of rotation of vortices which are created by ribs in the channel flow, the streamline projection on the plane perpendicular to the main flow is presented for simulations.

One can notice in Figures 7–8 that both the flow structure and the outlet stagnation pressure are properly predicted in numerical simulations, they very well agree with the experiment. However, for the channel of 1:4 AR the higher stagnation pressure areas in the experiment seem to be more intensive in relation to the CFD data. One can see in Figures 7–8 that the parallel setting of ribs creates two main vortices with the opposite sense of rotation in the flow. The other setting of ribs (crossing) creates a different flow pattern in the channel, *i.e.* two main vortices with the same sense of rotation, however, the flow direction in these two vortices is opposite in the channel centre. The sizes of vortices are very similar both in the basic channel with 1:4 AR and the higher channel (1:6 AR), therefore the zone with the higher uniform stagnation pressure and velocity has appeared in the middle space of this channel. There is no rotative movement of the flow in this zone. The velocity in the middle of the channel is higher than in the vicinity of the ribs (Figure 8). This indicates a lower drag in the channel centre and causes a decrease in the velocity of the vortices near the ribbed walls.

There are simply more mass flows where the drag is lower. In Figure 8a one can also notice the lower velocity difference between the core and periphery of the vortex in relation to the basic channel (Figure 7a) what affects the lower angular momentum of the vortex and may as consequence influence stresses on the wall in the higher channel.

Comparing the flow near the walls for two different rib settings, Figures 7b and 7d, one can observe that a weak circumferential motion comprising two dominant vortices for the crossing setting of ribs. However, at such channel proportion (AR = 1:4) this motion is rather weak in relation to the square channel (Figure 1b), but nevertheless the crossing setting of ribs shows some potential towards a decrease in losses and this solution can be considered for application in channels with lower cross section aspect ratios.

Figures 9–10 present the streamlines formed in the flow along the channels with different aspect ratios. The ribbed part of the channel starts from the coordinate at $X = 0$. As one can see the vortices size changes along the channel. At the beginning of ribbed section the vortices are small, then gradually enlarge towards the channel outlet and finally they are occupying almost the whole channel cross-section of a lower aspect ratio. This shows that the size of vortices depends rather on the channel width than on the channel height.

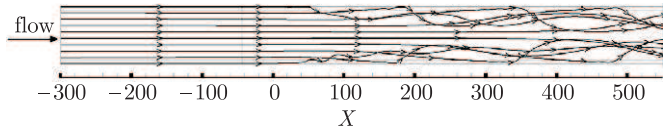

Figure 9. Streamlines along channel with 1:4 AR

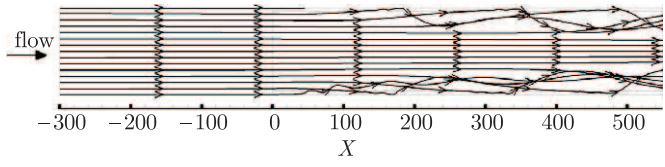

Figure 10. Streamlines along channel with 1:6 AR

In Table 2 losses at the ribbed channel outlet are shown. The losses are integrated on the whole plane at $X = 550$ in a range of $Y = -38$ to 38 and $Z = -9$ to 9 for 1:4 AR and in a range of $Y = -58$ to 58 for 1:6 AR. The loss coefficient ζ was calculated according to Equation (1), what means that losses of stagnation pressure are normalized by the dynamic component of the pressure.

$$\zeta = \frac{P_0 - P_P}{\frac{1}{2}\rho U^2} \tag{1}$$

where: $P_0 - P_P$ is the stagnation pressure difference between the inlet and the outlet, ϱ and U are the density and velocity at a particular point of the measurement plane.

Table 2. Loss coefficient at the ribbed channel outlet

	Flow case		
	Par-1:4	Cr-1:4	Par-1:6
Experiment	0.95	0.90	0.89
CFD	1.02	1.03	0.87

One can say that the loss coefficient in numerical simulations of the model turbine blade radial passage is properly predicted only for a channel of a higher aspect ratio. For the channel with 1:4 AR the numerical simulations show higher losses in relation to the experimental results. This corresponds to stagnation pressure distributions in Figures 7a and 7b, also 7c and 7d. In the experiment one can observe that the high stagnation pressure areas near the corners and TE wall have higher values than in CFD, what means higher velocity and lower losses as shown in Table 2. Probably the turbulence model introduces too large dissipation in numerical simulations for the channel with the lower aspect ratio where the mixing processes are more intensive than in the higher channel.

Based on Table 2 (Exp) one can see the tendency towards losses decreasing in case of both the crossing rib configuration and the channel higher aspect ratio. Such results show a potential towards a decrease in losses for both directions of channel modification. A higher potential can be predicted for crossing ribs, especially for lower aspect ratios (even lower than 1:4), because in this case there is little risk in the heat transfer reduction. For the high channel AR (1:6) such risk exists because the influence on wall stresses was observed and in consequence it may occur that decreasing losses may be accompanied also by heat exchange reduction.

5. Conclusions

A new test section was developed and designed to obtain a similar flow pattern as in the reference inner cooled channel of a turbine blade. The test channel has the same aspect ratio and shape of ribs. The following conclusion can be drawn from the above described investigations:

- A model of an internal cooling channel of a gas turbine blade was manufactured and equipped with the necessary systems for aerodynamic measurement;
- Computational mesh and a numerical model were prepared for all cases of experimental flow cases;
- Ribs on the suction and pressure side walls create a specific flow structure with two dominant vortices along the channel with the sense of rotation depending on the rib configuration;
- Two modifications of a basic channel, both the crossing rib configuration and the channel higher aspect ratio, show a tendency towards decreasing losses;
- A change of the rib configuration shows little effect on the decrease in pressure losses in the channel with the 1:4 aspect ratio, this solution can be more efficient for lower aspect ratios;

- An increase in the channel aspect ratio provides a decrease in pressure losses, however, with this solution there is a risk of heat exchange reduction;
- The flow structure in a numerical simulation is very similar to the measured one, but the pressure losses in lower aspect ratio channels are higher in relation to the experiment. Probably the k-ω SST turbulence model does not predict with sufficient accuracy the dissipations processes in such a complex flow formed in the vicinity of the ribs. Another source of discrepancies between the numerical simulations and the experiment is a different boundary layer at the ribbed section inlet, what also additionally influences the development of different secondary flows.

Acknowledgements

The research leading to these results received funding from the European Union Seventh Framework Programme (FP7/2007–2013) under Grant Agreement No. 233 799 (ERICKA).

The CFD research was supported by CI TASK and in part by PL-Grid Infrastructure.

References

[1] Metzger D E and Larson D E 1986 *ASME J. Heat Transfer* **96** 459
[2] Kim R, Mochizuki S and Murata A 2001 *ASME J. Heat Transfer* **123** 675
[3] Arts T, Benocci C and Rambaud P 2007 *3rd International Symposium on Integrating CFD and Experiments in Aerodynamics*, U. S. Air Force Academy
[4] http://www.ericka.eu
[5] Cakan M 2000 *Aero-thermal Investigation of Fixed Rib-roughened Internal Cooling Passages, Ph.D. Thesis*, Turbomachinery Department, Von Karman Institute for Fluid Dynamics